

# Electron Transfer Methods in Open Systems

Nicolas Bergmann<sup>†</sup> and Michael Galperin<sup>\*,‡</sup>

<sup>†</sup>*Department of Chemistry, Technical University of Munich, D-85748 Garching, Germany*

<sup>‡</sup>*Department of Chemistry & Biochemistry, University of California San Diego, La Jolla,  
CA 92093, USA*

E-mail: micalgalperin@ucsd.edu

Phone: +1 858 246 0511

## Abstract

Utilization of electron transfer methods for description of quantum transport is popular due to simplicity of the formulation and its ability to account for basic physics of electron exchange between system and baths. At the same time, necessity to go beyond simple golden rule-type expressions for rates was indicated in the literature and *ad hoc* formulations were proposed. Similarly, kinetic schemes for quantum transport beyond usual second order Lindblad/Redfield considerations were discussed. Here we utilize recently introduced by us nonequilibrium Hubbard Green's functions diagrammatic technique to analyze construction of rates in open systems. We show that previous considerations for rates of second and fourth order can be obtained as a particular case of zero and second order Green's function diagrammatic series with bare diagrams. We discuss limitations of previous considerations, stress advantages of the Hubbard Green's function approach in constructing the rates and indicate that standard dressing of the diagrams is a natural way to account for additional baths/degrees of freedom when formulating generalized expressions for the rates.

# Introduction

Electron transfer processes are the heart of oxidation-reduction reactions which play important role in chemistry and biology.<sup>1-3</sup> Theoretical description of electron transfer rates at the level of the Marcus theory<sup>4-10</sup> is widely utilized for the description of variety of phenomena from photovoltaics, batteries design and catalysis in chemistry<sup>11-16</sup> to photosynthesis, vision and sense of smell in biology.<sup>17-23</sup>

Interfacial electron transfer is behind many vital biological processes.<sup>24-28</sup> Recently, biomolecules were utilized as building blocks in electric circuits. Biomolecular junctions are useful as a tool to study properties of molecules and as potential bioelectronic devices. For example, electron transport was measured through DNA,<sup>29-31</sup> oligopeptides<sup>32,33</sup> and electron transfer proteins.<sup>34-36</sup> Also, STM junctions were suggested as a convenient tool for DNA detection and sequencing.<sup>37</sup>

Traditionally, electron transfer theory considers isolated donor-bridge-acceptor systems. Nevertheless, this theoretical approach appears to be useful also in description of electron transport in open molecular systems such as, e.g., redox molecular junctions.<sup>38-41</sup> Formal relationship between electron transfer rates and molecular conduction was discussed in the literature.<sup>42</sup>

In both intra-system and interfacial processes in condensed phase electron transfer may be assisted by intermediates. For example, intermediate states play important role in photovoltaic<sup>43</sup> or long-range DNA electron transfer processes.<sup>44-46</sup> Effects of intermediates on electron transfer are often discussed in terms of super-exchange vs. hopping mechanism. Clearly, the two mechanisms are limiting cases (coherent and completely incoherent) of the same process, and attempts to unify electron transfer rate expression were done in the literature.<sup>47,48</sup> However, these attempts are *ad hoc* perturbation theory considerations, and an ordered way of rate simulations is still lacking.

Constructing generalized expressions for rates is also at the heart of kinetic equations approaches to transport. For example, Refs. 49,50 are similar in the spirit effort to introduce

a scheme for constructing generalized expressions for rates. Advantage of this approach is possibility to account for higher order processes in system-bath couplings in an ordered way of bare perturbation theory. Still, questions of, e.g., accounting for additional degrees of freedom (such as other baths) within a particular order in the system-primary baths coupling remains open. Also, the methodology has usual for quantum master equations restriction of applicability only in the high temperature regime (thermal energy should be big relative to characteristic energy of the system-bath coupling). We note in passing that in interacting open systems kinetic schemes should be applied with caution.<sup>51</sup>

Nonequilibrium Green's functions (NEGF)<sup>52</sup> is a tool capable to describe both superexchange and hopping transport regimes, as well as smooth transition between the two limiting cases. Diagrammatic perturbation theory is a way to account for interaction with intermediate (or additional) degrees of freedom in an ordered form. Also, Green's function considerations are applicable in any temperature regime. However, identifying rates is not possible within the standard NEGF.

Here, we show that recently introduced by us many-body NEGF flavor, the Hubbard NEGF,<sup>53</sup> while retaining advantages of the Green's function methods is capable to provide connection with kinetic schemes. So that ordered construction of generalized rates becomes possible employing the Hubbard Green's function diagrammatic technique. Structure of the paper is the following. After introducing junction model we give a short overview of the Hubbard NEGF introducing conceptual details not presented in its original introduction in Ref. 53. After this we present connection between the Hubbard NEGF and kinetic schemes of Refs. 49,50 showing a way to formulate rates within the Hubbard NEGF. We conclude by discussing advantages of Green's functions formulation and outlining directions for future research.

# Model

We consider generic model of a junction which consists of a molecule,  $M$ , coupled to two contacts,  $L$  and  $R$ . Depending on particular problem, molecular (system) part can describe electronic, vibrational, optically-dressed (e.g. polariton) or any other degrees of freedom. We assume that quantum chemistry problem for the isolated system has been solved, and many-body eigenstates  $|S\rangle$  and their energies  $E_S$  are known. We note in passing that even in systems with very big (or even infinite) number of many-body eigenstates, energetics of the junction (bias, driving laser field, etc.) allows to identify a finite subset, which is enough for first principles simulation of experimental data for realistic systems.<sup>54–58</sup> Contacts (baths) are assumed to be reservoirs of free charge carriers each at its own equilibrium. Second quantization is utilized to treat baths' degrees of freedom. This is minimal model for discussion of electron transfer rates within the Hubbard NEGF. Additional baths and/or degrees of freedom (e.g., phonons) can be added to the consideration in a straightforward manner.

Hamiltonian of the minimal model is

$$\hat{H} = \hat{H}_M + \sum_{K=L,R} \left( \hat{H}_K + \hat{V}_{MK} \right) \quad (1)$$

$$\hat{H}_M = \sum_{S \in M} |S\rangle E_S \langle S| \quad (2)$$

$$\hat{H}_K = \sum_{k \in K} \varepsilon_k \hat{c}_k^\dagger \hat{c}_k \quad (3)$$

$$\hat{V}_{MK} = \sum_{S_1, S_2 \in M} \sum_{k \in K} \left( V_{k, S_1 S_2} \hat{c}_k^\dagger |S_1\rangle \langle S_2| + H.c. \right) \quad (4)$$

Here  $\hat{H}_M$  and  $\hat{H}_K$  ( $K = L, R$ ) are molecule and contacts Hamiltonians, and  $\hat{V}_{MK}$  introduces system-baths coupling.  $\hat{c}_k^\dagger$  ( $\hat{c}_k$ ) creates (annihilates) electron in single-electron state  $k$  in the contacts.  $V_{k, S_1 S_2}$  is matrix element for electron transfer from system to bath in which system goes from state  $|S_2\rangle$  to  $|S_1\rangle$ .

Below we will be interested in electron flux through the junction and corresponding intra-system electron transfer rates. Note that while we focus on charge current, the consideration is more general and can equivalently be applied to calculation of any other intra-system rates (e.g., related to photon or energy flux) or to multi-time correlation functions as employed in, e.g., nonlinear optical spectroscopy.<sup>59</sup>

## Hubbard NEGF

Central object of interest is the single particle Hubbard Green's function, which is defined on the Keldysh contour as

$$G_{S_1 S_2, S_3 S_4}(\tau, \tau') = -i \langle T_c \hat{X}_{S_1 S_2}(\tau) \hat{X}_{S_3 S_4}^\dagger(\tau') \rangle \quad (5)$$

Here  $X_{S_1 S_2} \equiv |S_1\rangle\langle S_2|$  is the Hubbard (or projection) operator,  $T_c$  is the contour ordering operator, and  $\tau$  and  $\tau'$  are the contour variables. Advantage of the Hubbard over standard NEGF for our study is possibility to access information on many-body states of the system. As we show below, this moment is crucial for formulating general expressions for rates within the Green's function methodology.

Historically, Hubbard Green's functions were introduced for treatment of strongly correlated extended (lattice type) equilibrium systems in Ref. 60. Diagrammatic technique (expansion around atomic limit) for such equilibrium Green's functions<sup>61,62</sup> is based on assumption of equilibrium character of the uncoupled system's density operator

$$\hat{\rho}_0 = \frac{1}{Z_0} e^{-\hat{H}_0/k_B T}; \quad Z_0 = \text{Tr} e^{-\hat{H}_0/k_B T} \quad (6)$$

At nonequilibrium, Hubbard Green's functions were used for transport simulations employing relations derived from equation-of-motion considerations and functional derivatives in auxiliary fields.<sup>63–68</sup> While the latter approach is very useful, it lacks rigor of ordered

diagrammatic expansion and provides only vague rules about choice of auxiliary fields and terms resulting from performing functional derivatives.

Recently, we introduced nonequilibrium version of the Hubbard diagrammatic technique<sup>53</sup> making it applicable to nonequilibrium impurity-type (molecular junction) problems. Contrary to original lattice type formulation, we introduce baths and utilize state representation only for the system, while bath degrees of freedom are treated within standard second quantization. Thus, perturbative expansion in the system-baths couplings in each order yields product of two multi-time correlation functions: one for the system and one for the bath operators (see Ref. 53 for details). Because baths are assumed to be non-interacting, the latter can be treated using the standard Wick's theorem. To evaluate multi-time correlation function of Hubbard (system) operators we employ usual for NEGF assumption of steady-state being independent of initial condition at infinite past. Thus, assuming equilibrium initial system state, Eq. (6), correlation function of Hubbard operators is evaluated using diagrammatic technique of Refs. 61,62. As a result, Hubbard NEGF appears to be a modified (by presence of baths and nonequilibrium character of the system) version of the lattice diagrammatic technique (see Ref. 53 for details). The technique appears to be quite stable over wide range of parameters,<sup>69</sup> helpful in evaluation of electronic friction in junctions,<sup>70,71</sup> and useful as a convenient tool in first principles simulations of optoelectronic devices.<sup>56–58</sup>

It is important to realize, however, that requirement of equilibrium character of the uncoupled system density operator, Eq. (6), in principle can be relaxed. Indeed, diagrammatic technique of Refs. 61,62 is based on commutation properties of the Hubbard operators (interaction representation)

$$\hat{X}_{S_1 S_2}(t) \hat{X}_{S_3 S_4}^\dagger(t') = e^{-i(E_{S_2} - E_{S_1})(t - t')} \delta_{S_2, S_4} \hat{X}_{S_1 S_3}(t') \pm \hat{X}_{S_3 S_4}^\dagger(t') \hat{X}_{S_1 S_2}(t) \quad (7)$$

with sign chosen according to the operators statistics (Bose or Fermi - see Ref. 53 for details)

and ability to interchange Hubbard and equilibrium density operators

$$\hat{X}_{S_1 S_2} \hat{\rho}_0 = \hat{\rho}_0 \hat{X}_{S_1 S_2} e^{(E_{S_1} - E_{S_2})/k_B T} \quad (8)$$

Thus, it is clear that diagrammatic technique for the Hubbard operators can be equivalently formulated for any form of system's density operator as long as the latter is a function of molecular (system) Hamiltonian only

$$\hat{\rho}_0 = f(\hat{H}_M) \equiv \sum_S |S\rangle f(E_S) \langle S| \quad (9)$$

While this observation does not change numerical procedure for the Hubbard NEGF, it yields two important conceptual consequences. First, the Hubbard NEGF can be considered as a natural tool for expansion around results of a quasi-particle-type consideration performed in the basis of many-body states capable to introduce states broadening and bath-induced coherences, which were missed in the latter. For example, such quasi-particle-type consideration is the Markov Redfield/Lindblad quantum master equation. In this case  $f(E_S)$  in (9) is probability  $P_S$  of state  $|S\rangle$  to be observed. Second, considering situation where only one state is populated,  $P_S = 1$ , nonequilibrium diagrammatic technique for Hubbard Green's functions provides access to traditional expressions for rates of transitions from state  $|S\rangle$  to all other states of the system. Below we discuss details of this Green's function-to-kinetic scheme connection.

## Connection to kinetic schemes

We now turn to discuss how Hubbard NEGF can be used to define generalized expressions for transfer rates. We explore connection to the kinetic scheme presented in Refs. 49,50, thus identifying rate expressions in terms of the Hubbard NEGF, and indicate how the rates expressions can be generalized.



We start by considering equation-of-motion for the probability of state  $|S\rangle$  to be observed (Heisenberg picture)

$$P_S(t) \equiv \langle \hat{X}_{SS}(t) \rangle \quad (10)$$

under driving by the Hamiltonian  $\hat{H}$  of (1). Writing Heisenberg equation of motion for (10) and using standard NEGF derivation (similar to the derivation leading to the celebrated Meir-Wingreen expression for current<sup>52</sup>) one gets

$$\begin{aligned} \frac{d}{dt} P_S(t) = 2\text{Re} \sum_{S_1, S_2, S_3} \int_{-\infty}^t dt' & \\ \left( \sigma_{SS_3, S_1 S_2}^>(t-t') G_{S_1 S_2, SS_3}^<(t'-t) - \sigma_{SS_3, S_1 S_2}^<(t-t') G_{S_1 S_2, SS_3}^>(t'-t) \right. & \quad (11) \\ \left. - \sigma_{S_3 S, S_1 S_2}^>(t-t') G_{S_1 S_2, S_3 S}^<(t'-t) + \sigma_{S_3 S, S_1 S_2}^<(t-t') G_{S_1 S_2, S_3 S}^>(t'-t) \right) & \end{aligned}$$

Here  $G^{<(>)}$  is the lesser (greater) projection of the Hubbard Green function (5) and  $\sigma^{<(>)}$  is the lesser (greater) projection of the self-energy due to coupling to contacts  $L$  and  $R$

$$\sigma_{S_1 S_2, S_3 S_4}(\tau, \tau') = \sum_{K=L, R} \sum_{k \in K} V_{S_1 S_2, k} g_k(\tau, \tau') V_{k, S_3 S_4} \equiv \sum_{K=L, R} \sigma_{S_1 S_2, S_3 S_4}^K(\tau, \tau') \quad (12)$$

where  $g_k(\tau, \tau') = -\langle T_c \hat{c}_k(\tau) \hat{c}_k^\dagger(\tau') \rangle$  is the Green function of free electron in single-particle state  $k$ .

Expression (11) is exact, and our goal is to represent it in the form of rate equation, which will allow to identify expressions for the rates. Following Refs. 49,50 we will be interested in rates of second and fourth order in the system-baths couplings. Taking into account that Hubbard NEGF diagrammatic technique expands in system-baths coupling and noting that second order in the coupling already enters (11) via self-energy (12), it is natural to expect that second order rates should result from zero order of the Hubbard GFs expansion, while fourth order rates should be accessible from second order of the Hubbard NEGF diagrammatic series.

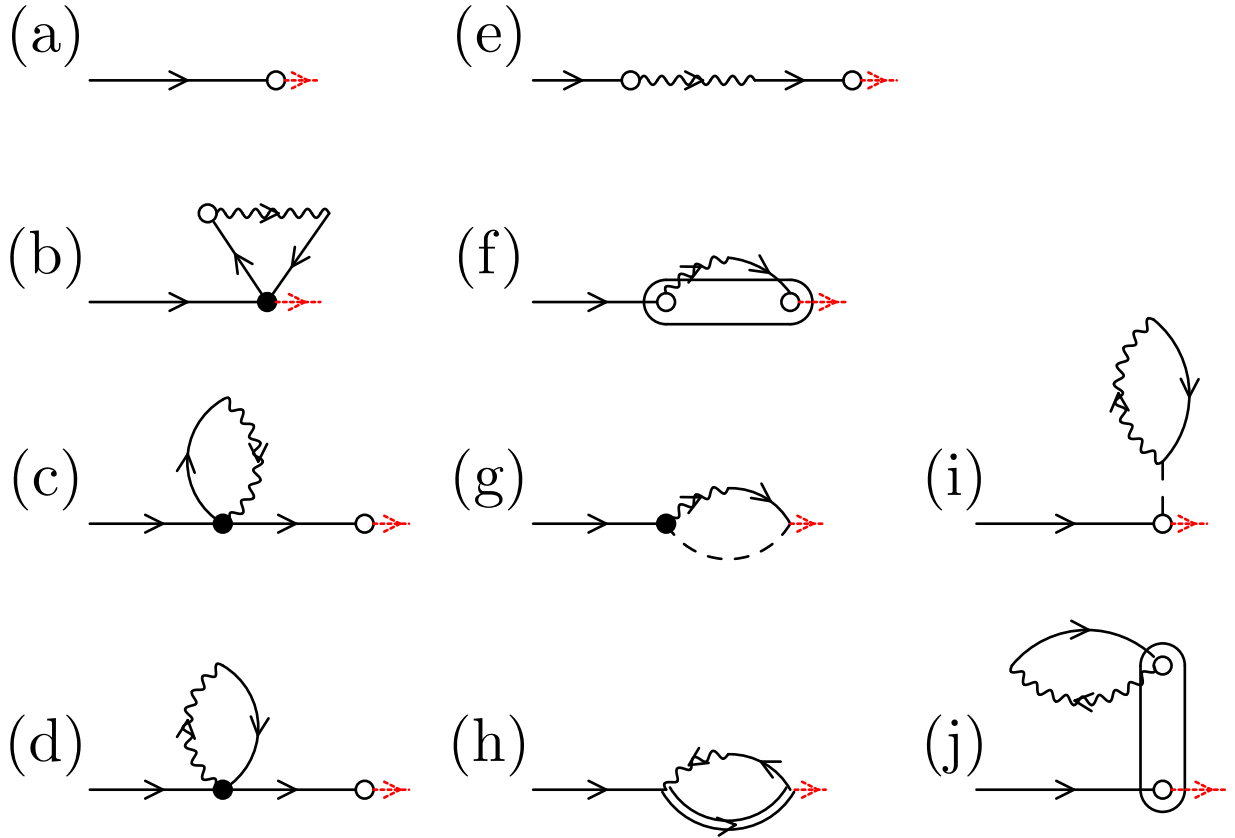


Figure 1: Diagrams of the Hubbard NEGF (5) expansion in system-baths coupling. Shown are (a) zero and (b-j) second order diagrams. See text for details.

Figure 1 shows diagrams of zero (panel a) and second (panels b-j) order expansion in the system-bath coupling. Directed straight and wavy lines represent Fermion propagator  $g_m(\tau, \tau')$  and self-energy  $\sigma_{mm'}(\tau, \tau')$ , Eq. (12), respectively. Here  $m \equiv S_1 S_2$  is single electron transition between pair of many-body states  $|S_1\rangle$  and  $|S_2\rangle$ , i.e.  $N_{S_1} + 1 = N_{S_2}$  ( $N_S$  is number of electrons in state  $|S\rangle$ ). Dashed line stands for Boson propagator  $g_b(\tau, \tau')$  in the same charging block, i.e.  $b \equiv S_1 S_2$  with  $N_{S_1} = N_{S_2}$ . Directed double line represents two-electron propagator  $d_b(\tau, \tau')$ , where  $b \equiv S_1 S_2$  with  $N_{S_1} + 2 = N_{S_2}$ . Empty circle stands for (zero-order) spectral weight

$$\langle \hat{F}_{m_1 m_2}(\tau) \rangle_0 \equiv \langle \{ \hat{X}_{m_1}(\tau); \hat{X}_{m_2}^\dagger(\tau) \} \rangle_0 \quad (13)$$

and oval with two circles is correlation function

$$\langle \delta \hat{F}_{m_1 m_2}(\tau) \delta \hat{F}_{m_3 m_4}(\tau') \rangle_0 \quad (14)$$

where  $\delta \hat{F}_{mm'} = \hat{F}_{mm'} - \langle \hat{F}_{mm'} \rangle_0$ . Filled circles stand for ‘pruned’ vertices.<sup>62</sup> Finally, red dashed line indicates the end point of the diagram. For more details see Ref. 53.

We note that Fig. 1 presents bare diagrams. As discussed in the previous section, the Hubbard NEGF may be considered as expansion around results of the Markov Redfield/Lindblad quantum master equation. Assuming we are dealing with such an expansion, each diagram can be easily represented in terms of state probabilities. For example, lesser and greater projections of the Fermion propagator  $g_m(\tau, \tau')$  are ( $m \equiv S_1 S_2$  with  $N_{S_1} + 1 = N_{S_2}$ )

$$g_m^<(t - t') = i \frac{P_{S_2}}{P_{S_1} + P_{S_2}} e^{-i(E_{S_2} - E_{S_1})(t - t')} \quad (15)$$

$$g_m^>(t - t') = -i \frac{P_{S_1}}{P_{S_1} + P_{S_2}} e^{-i(E_{S_2} - E_{S_1})(t - t')} \quad (16)$$

while its casual and anti-casual projections are

$$g_m^c(t-t') = \theta(t-t')g_m^>(t-t') + \theta(t'-t)g_m^<(t-t') \quad (17)$$

$$g_m^{\bar{c}}(t-t') = \theta(t-t')g_m^<(t-t') + \theta(t'-t)g_m^>(t-t') \quad (18)$$

Similarly one can evaluate other elements of the diagrams, and represent the diagrams in terms of states probabilities  $P_S$  and time-dependent factors.

We now turn to order-by-order analysis of the diagrams. Before discussing the contributions we have to stress difference in Green function (Hilbert space) and quantum master equation (Liouville space) languages mentioned also in our previous publication:<sup>72,73</sup> time arrangements on the Keldysh contour called diagrams in the QME language are projections in the language of GFs. The difference is of minor importance for the zero-order contribution, because the latter has only one diagram (see Fig. 1a). However, as is discussed later, it becomes critical for understanding higher order contributions and connection between the methods.

## Zero-order contributions

Zero-order contribution to the Hubbard GF (5) is

$$G_{mm'}^{(0)}(\tau, \tau') = g_m(\tau, \tau') \langle \hat{F}_{mm'}(\tau') \rangle_0 \quad (19)$$

Here  $m = S_1 S_2$  and  $m' = S_3 S_4$  with  $N_{S_1} + 1 = N_{S_2}$  and  $N_{S_3} + 1 = N_{S_4}$ . We note that there are four different projections of (19) contributing to (11) - one projection for each one of the terms on the right side of the expression. The projections are given in Fig. 2. Note there are eight projections when considering also complex conjugates taken into account by  $2 \text{Re} \dots$  in (11) - those are obtained by interchanging time positions between contour branches and flipping arrows.

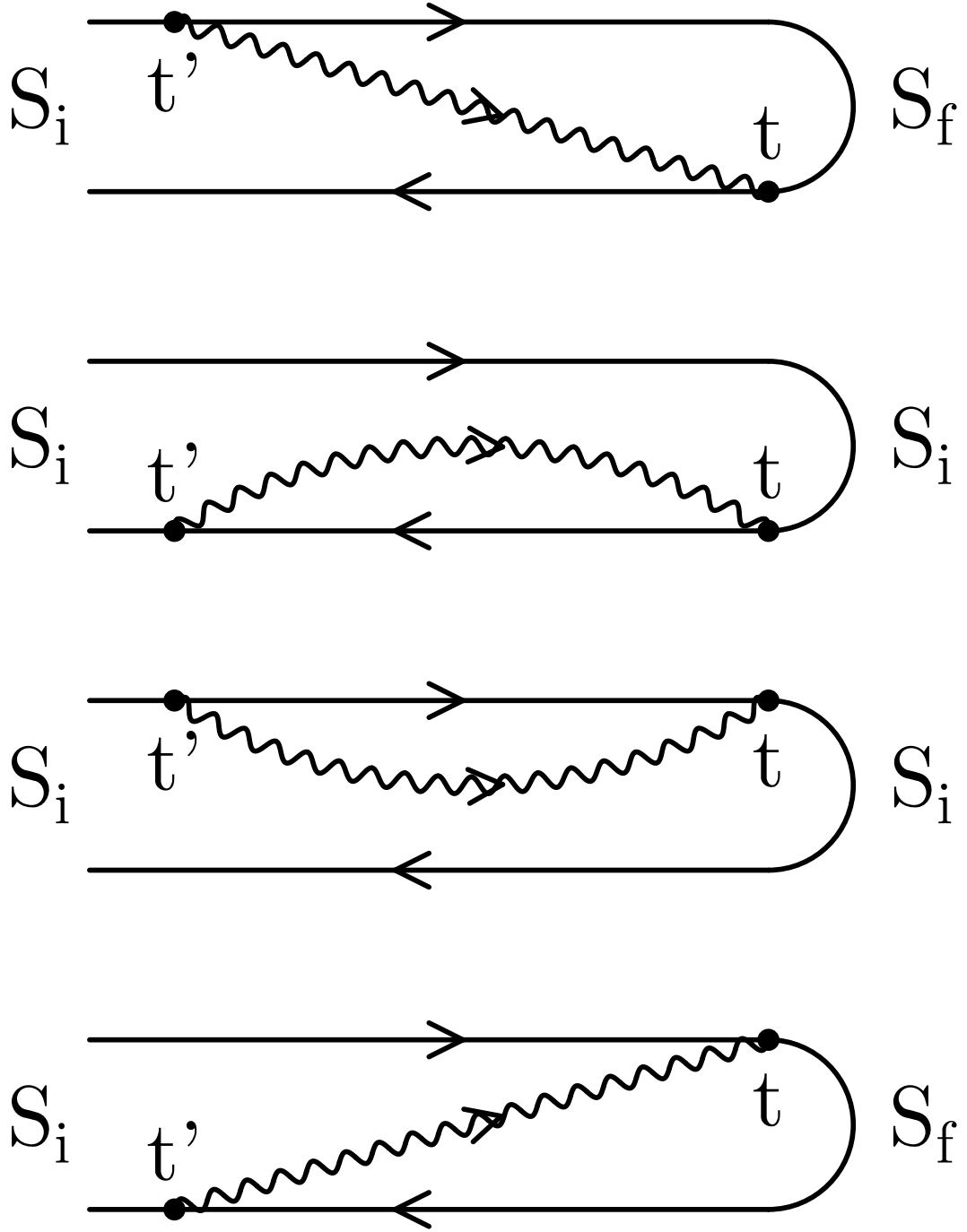


Figure 2: Projections of the zero-order contribution, diagram in Fig. 1a, to equation-of-motion (11): the four projections correspond to the four terms in the right side of the expression.

Taking projections of Eq. (19) on the Keldysh contour, substituting zero-order expressions for the locator and spectral weight, Eqs. (15)-(18), and utilizing the results in Eq. (11) yields expressions for the second order transfer rates from initial state  $|S_i\rangle$  to final state  $|S_f\rangle$  (see Supporting Information for details)

$$W_{S_f \leftarrow S_i}^{(2)} = i \sigma_{S_f S_i, S_f S_i}^> (E_{S_i} - E_{S_f}) - i \sigma_{S_i S_f, S_i S_f}^< (E_{S_f} - E_{S_i}) \quad (20)$$

As expected, these are golden rule type expressions. We note in passing that while considering contributions in Eq. (11) from different terms it is enough to account for rates appearing in front of  $P_{S_i}$  with  $S_i \neq S_f$ , because rates of the type  $S_i \leftarrow S_i$  (given by second and third projections in Fig. 2) can be obtained from the normalization condition

$$\sum_{S_f} W_{S_f \leftarrow S_i} = 0 \quad (21)$$

The latter is easy to check also by direct evaluation of the rates.

## Second order contributions

Diagrams of second order contributions to the Hubbard GF (5) are shown in panels (b)-(j) of Fig. 1. Their explicit expressions are (letters next to expressions correspond to diagrams

in Fig. 1)

$$\begin{aligned}
G_{mm'}^{(2)}(\tau, \tau') &= \sum_{m_1, m_2} \int_c d\tau_1 \int_c d\tau_2 \sigma_{m_1 m_2}(\tau_1, \tau_2) \times & (22) \\
&\left( \begin{aligned}
&-i g_m(\tau, \tau') \gamma(m_2, mm') g_\gamma(\tau', \tau_1) \langle \hat{F}_{\gamma m_1}(\tau_1) \rangle_0 g_{m_2}(\tau_2, \tau' +) & (b) \\
&+ i g_m(\tau, \tau_2) g_{m_1}(\tau_2, \tau_1) \gamma(\tilde{m}_1, m\tilde{m}_2) g_\gamma(\tau_2 -, \tau') \langle \hat{F}_{\gamma m'}(\tau') \rangle_0 & (c) \\
&+ i g_m(\tau, \tau_1) g_{m_2}(\tau_2, \tau_1 +) \gamma(m_2, mm_1) g_\gamma(\tau_1, \tau') \langle \hat{F}_{\gamma m'}(\tau') \rangle_0 & (d) \\
&+ g_m(\tau, \tau_1) \langle \hat{F}_{mm_1}(\tau_1) \rangle_0 g_{m_2}(\tau_2, \tau') \langle \hat{F}_{m_2 m'}(\tau') \rangle_0 & (e) \\
&+ g_m(\tau, \tau_1) \langle T_c \delta \hat{F}_{mm_1}(\tau_1) \delta \hat{F}_{m_2 m'}(\tau_2) \rangle_0 g_{m_2}(\tau_2, \tau') & (f)+(g) \\
&+ g_m(\tau, \tau_2) \langle T_c \delta \hat{F}_{m\tilde{m}_2}(\tau_2) \delta \hat{F}_{\tilde{m}_1 m'}(\tau') \rangle_0 g_{m_1}(\tau', \tau_1) & (h) \\
&- g_m(\tau, \tau') \langle T_c \delta \hat{F}_{mm'}(\tau') \delta \hat{F}_{m_2 m_1}(\tau_1) \rangle_0 g_{m_2}(\tau_2, \tau_1) & (i)+(j)
\end{aligned} \right)
\end{aligned}$$

Here  $\tau -$  ( $\tau +$ ) indicates contour variable right before (after)  $\tau$  in contour ordering sense,  $\tilde{m} = S_2 S_1$  for  $m = S_1 S_2$ , and  $\gamma$  is defined via  $\gamma(m_1, m_2 m_3) \hat{X}_\gamma \equiv [\hat{X}_{m_1}; \hat{F}_{m_2 m_3}]$ .

Second order brings into consideration two more contour variables,  $\tau_1$  and  $\tau_2$ , thus increasing number of projections. Moreover, Green function projections account only for ordering of the variables on the Keldysh contour, while QME keeps track also on ordering along real time axis. So, one Green function projection corresponds to several QME projections.<sup>72,74</sup> With four contour variables ( $\tau$ ,  $\tau'$ ,  $\tau_1$ , and  $\tau_2$ ) and with restriction of  $\tau$  (as variable representing the signal) being the latest time on real time axis (causality principle) one has to account for 48 QME projections. Note, without  $2 \text{Re} \dots$  term in (11) number of QME projections doubles:  $3!$  orderings of times  $t'$ ,  $t_1$  and  $t_2$  on the real time axes multiplied with  $2^4$  variants of distribution of the four variables on branches of the contour. Each of terms in the right side of (11) yields 12 QME projections, and each QME projection has contributions from several GF diagrams of Fig. 1(b)-(j).

Figure 3 shows the projections distributed following Ref. 50 into three topologically different classes (**A**, **B**, **C**) with three groups within each class (**(0)**, **(1)** and **(2)** - minimum

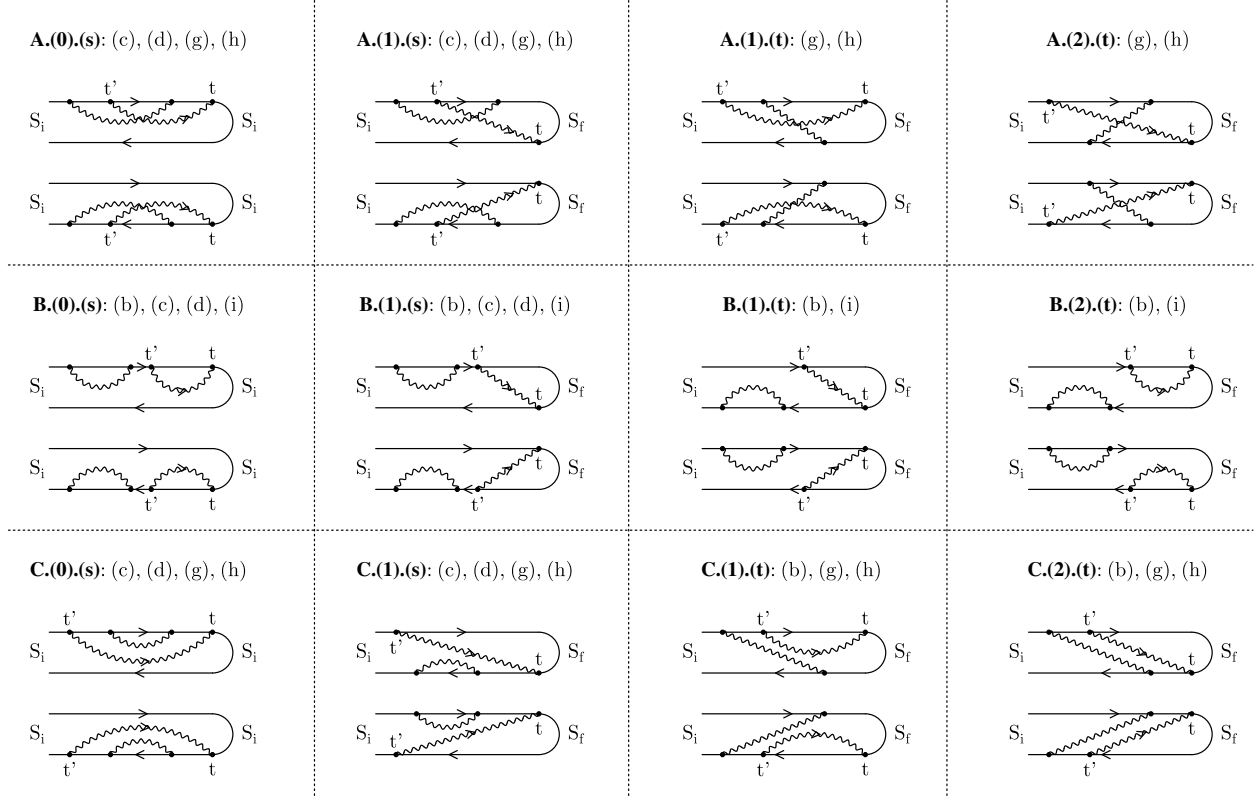


Figure 3: Projections of the second-order contributions, diagrams in Figs. 1(b)-(j), to equation-of-motion (11). Following Ref. 50 the projections are classified by 3 topologically different classes (**A**, **B**, **C**), three groups ((**0**), (**1**), (**2**)) and two sub-groups ((**s**) and (**t**)). Letters (b)-(j) correspond to second order diagrams from Fig. 1 contributing to the projections. See text for details.



number of times on either branch of the contour) and with standalone ((s)) or triple ((t)) subgroups defined by number of different positions latest time (except  $t$ , which is always the latest) can have relative to other times on the contour without changing projection topology. For simplicity, in each case we draw only one projection with latest time being at the extreme right and did not indicate directions of self-energy line corresponding to variables  $\tau_1$  and  $\tau_2$ , so that for the self-energy depending on directions of arrows two different projections can be obtained from the one given in Fig. 3. As mentioned above, complex conjugate analogs of the considered diagrams are obtained by inter-changing times between branches and flipping directions of lines. We also indicate which of the diagrams from Fig. 1(b)-(j) contribute to each of the classes/groups/subgroups. Substituting (22) into (11) yields expressions for the fourth order transfer rates. Explicit expressions for the rates are given in the Supporting Information.

Comparing Hubbard NEGF approach to building transfer rates with the kinetic procedure introduced in Refs. 49,50 leads to several important observations as follows. First, Hubbard NEGF diagrammatic technique naturally takes care of disregarding disconnected diagrams, so that no additional special consideration is required. Second, for dressed diagrams (see discussion in the next section) artificial separation of the contributions into secular and non-secular parts (depending on energy differences between pairs of states corresponding to transition relative to thermal energy) is not needed either. Third, fourth order transfer rates built from bare expansion miss contributions from diagrams (e), (f), and (j) of Fig. 1. The omission is natural because diagram (e) is responsible for deviations from steady-state (accumulation or depletion of electrons in the system), which is absent at steady-state considered in Refs. 49,50. Diagrams (f) and (j) contain functions (14) which account for correlations between different states of the system. The latter are absent when rates are derived assuming independent (one-at-a-time) state population. Fourth, diagrams of Fig. 1 provide clear physical picture of transfer processes. For example, diagram (g) is responsible for co-tunneling, while diagram (h) describes two-electron transport. We stress

that it is diagrams (not projections) which are primary sources for the observed transfer characteristics. Finally, combination of projections in order to simplify evaluation of rates discussed in Ref. 50 is equivalent to change of consideration from QME-type projections, where real-time ordering is important, to GF-type projections, where only ordering along the contour matters. As indicated above, number of the latter projections is much smaller. These observations indicate that GF based approach to building transfer rates is simpler and more efficient. In the next section we also argue that GFs also provide an easy way to generalizations.

## Dressed rates

Standard Green function diagrammatic procedure prescribes to dress the expansion diagrams thus collecting a bare expansion into a resummed equation-of-motion. For the Hubbard NEGF this leads to modified Dyson equation.<sup>53,62</sup> However, full dressing makes transfer rates language obsolete. Thus, to go beyond bare expansion while still keeping kinetic scheme we propose to dress those diagram projections, which were identified as contributing to rates in the bare diagrammatic expansion. Technically, this means substituting zero-order expressions, Eqs. (15)-(18) for locators, spectral weights and correlation functions in the rates, with corresponding dressed expressions (see Ref. 53 and Supplementary Information for details). We note that while dressing one should be careful to not introduce double counting. The dressing can be performed with respect to the same system-bath interaction in which original expansion was performed, or with respect to interaction with other degrees of freedom/baths, or both. Note that GF diagrammatic technique rules allow to account for additional interactions in an ordered manner. This is contrary to *ad hoc* extensions considered in Refs. 47,48.

## Conclusion

We present Green function perspective on utilization of electron transfer techniques in description of quantum transport. Central role in the former is played by transfer rates, which are usually evaluated at the golden rule level of theory. Necessity to generalize such rate expressions to account for intermediates was indicated and *ad hoc* extension was formulated in Refs. 47,48. Similarly, kinetic schemes employing rates beyond second order in system-baths coupling were discussed in Refs. 49,50.

We indicate that Green's function method is a natural way to account for intermediates and go to any order in perturbative expansion in a well controlled way of diagrammatic expansion. However, inability to access system state resolved information in the standard NEGF does not allow to establish connection between its diagrammatic expansion and rates utilized in kinetic schemes. At the same time, the Hubbard NEGF theory, recently introduced by us,<sup>53</sup> yields such a possibility.

Utilizing zero-order (undressed) perturbation expansion of the Hubbard NEGF up to second order in the system-bath coupling we establish connection with expressions of second and fourth order expressions for the rates introduced in Refs. 49,50. We discuss connection between the two approaches and indicate advantages of Green's function techniques in deriving expressions for the rates. Finally, we note that standard dressing of diagrams in Green's function expansions yields a possibility of formulating generalized (dressed) expressions for rates capable to account for additional baths (degrees of freedom) in a well controlled ordered manner. Practical application of the theory to realistic simulations is a goal for future research.

## Acknowledgement

This material is based upon work supported by the National Science Foundation under CHE-1565939.

## Supporting Information Available

The following files are available free of charge. The Supporting Information is available free of charge on the ACS Publications website at DOI: XXX

Explicit expressions for second and fourth order transfer rates.

## References

- (1) Newton, M. D.; Sutin, N. Electron Transfer Reactions in Condensed Phases. *Ann. Rev. Phys. Chem.* **1984**, *35*, 437–480.
- (2) Kuznetsov, A. M. *Charge Transfer in Physics, Chemistry and Biology: Physical Mechanisms of Elementary Processes and an Introduction to the Theory*; Gordon & Breach, 1995.
- (3) Jortner, J.; Bixon, M. *Electron Transfer - from Isolated Molecules to Biomolecules*; John Wiley, 1999.
- (4) Marcus, R. A. On the Theory of Oxidation-Reduction Reactions Involving Electron Transfer. I. *J. Chem. Phys.* **1956**, *24*, 966–978.
- (5) Marcus, R. A. Electrostatic Free Energy and Other Properties of States Having Nonequilibrium Polarization. I. *J. Chem. Phys.* **1956**, *24*, 979–989.
- (6) Levich, V. G.; Dogonadze, R. R. Theory of Radiationless Electron Transitions Between Ions in Solutions. *Doklady Akad. Nauk SSSR* **1959**, *124*, 123–126.
- (7) Levich, V. G.; Dogonadze, R. R. Adiabatic theory of electron-transfer processes in solutions. *Doklady Akad. Nauk SSSR* **1960**, *133*, 159–161.
- (8) Hush, N. S. Adiabatic Theory of Outer Sphere Electron-Transfer Reactions in Solution. *Trans. Faraday Soc.* **1961**, *57*, 557–580.

- (9) Hush, N. S. Homogeneous and Heterogeneous Optical and Thermal Electron Transfer. *Electrochimica Acta* **1968**, *13*, 1005–1023.
- (10) Jortner, J. Temperature Dependent Activation Energy for Electron Transfer Between Biological Molecules. *J. Chem. Phys.* **1976**, *64*, 4860–4867.
- (11) Miller, J. R.; Calcaterra, L. T.; Closs, G. L. Intramolecular Long-Distance Electron Transfer in Radical Anions. The Effects of Free Energy and Solvent on the Reaction Rates. *J. Am. Chem. Soc.* **1984**, *106*, 3047–3049.
- (12) Miller, J. R.; Beitz, J. V.; Huddleston, R. K. Effect of Free Energy on Rates of Electron Transfer Between Molecules. *J. Am. Chem. Soc.* **1984**, *106*, 5057–5068.
- (13) Kuharski, R. A.; Bader, J. S.; Chandler, D.; Sprik, M.; Klein, M. L.; Impey, Molecular Model for Aqueous Ferrous-Ferric Electron Transfer. *J. Chem. Phys.* **1988**, *89*, 3248–3257.
- (14) Barbara, P. F.; Meyer, T. J.; Ratner, M. A. Contemporary Issues in Electron Transfer Research. *J. Phys. Chem.* **1996**, *100*, 13148–13168.
- (15) Rosso, K. M.; M., D. Reorganization Energy Associated with Small Polaron Mobility in Iron Oxide. *J. Chem. Phys.* **2004**, *120*, 7050–7054.
- (16) Nitzan, A. *Chemical Dynamics in Condensed Phases*; Oxford University Press, 2006.
- (17) Kuki, A.; Wolynes, P. Electron Tunneling Paths in Proteins. *Science* **1987**, *236*, 1647–1652.
- (18) Beratan, D. N.; Betts, J. N.; Onuchic, J. N. Protein Electron Transfer Rates Set by the Bridging Secondary and Tertiary Structure. *Science* **1991**, *252*, 1285–1288.
- (19) Beratan, D. N.; Onuchic, J. N.; Winkler, J. R.; Gray, H. B. Electron-Tunneling Pathways in Proteins. *Science* **1992**, *258*, 1740–1741.

- (20) Stuchebrukhov, A. A. Tunneling Currents in Electron Transfer Reactions in Proteins. *J. Chem. Phys.* **1996**, *104*, 8424–8432.
- (21) Stuchebrukhov, A. A. Tunneling Currents in Electron Transfer Reaction in Proteins. II. Calculation of Electronic Superexchange Matrix Element and Tunneling Currents Using Nonorthogonal Basis Sets. *J. Chem. Phys.* **1996**, *105*, 10819–10829.
- (22) Brookes, J. C.; Hartoutsiou, F.; Horsfield, A. P.; Stoneham, A. M. Could Humans Recognize Odor by Phonon Assisted Tunneling? *Phys. Rev. Lett.* **2007**, *98*, 038101.
- (23) Brookes, J. C.; Horsfield, A. P.; Stoneham, A. M. The Swipe Card Model of Odorant Recognition. *Sensors* **2012**, *12*, 15709–15749.
- (24) McLendon, G.; Hake, R. Interprotein Electron Transfer. *Chemical Reviews* **1992**, *92*, 481–490.
- (25) Miyashita, O.; Okamura, M. Y.; Onuchic, J. N. Interprotein Electron Transfer from Cytochrome C2 to Photosynthetic Reaction Center: Tunneling Across an Aqueous Interface. *Proc. Nat. Acad. Sci.* **2005**, *102*, 3558–3563.
- (26) Nojiri, M.; Koteishi, H.; Nakagami, T.; Kobayashi, K.; Inoue, T.; Yamaguchi, K.; Suzuki, S. Structural Basis of Inter-Protein Electron Transfer for Nitrite Reduction in Denitrification. *Nature* **2009**, *462*, 117–120.
- (27) Xiong, P.; Nocek, J. M.; Vura-Weis, J.; Lockard, J. V.; Wasielewski, M. R.; Hoffman, B. M. Faster Interprotein Electron Transfer in a [Myoglobin, b5] Complex with a Redesigned Interface. *Science* **2010**, *330*, 1075–1078.
- (28) McGrath, A. P.; Laming, E. L.; Casas Garcia, G. P.; Kvansakul, M.; Guss, J. M.; Trewhella, J.; Calmes, B.; Bernhardt, P. V.; Hanson, G. R.; Kappler, U. et al. Structural Basis of Interprotein Electron Transfer in Bacterial Sulfite Oxidation. *eLife* **2015**, *4*, e09066.

- (29) Cohen, H.; Nogues, C.; Naaman, R.; Porath, D. Direct Measurement of Electrical Transport Through Single DNA Molecules of Complex Sequence. *Proc. Nat. Acad. Sci.* **2005**, *102*, 11589–11593.
- (30) Gohler, B.; Hamelbeck, V.; Markus, T. Z.; Kettner, M.; Hanne, G. F.; Vager, Z.; Naaman, R.; Zacharias, H. Spin Selectivity in Electron Transmission Through Self-Assembled Monolayers of Double-Stranded DNA. *Science* **2011**, *331*, 894–897.
- (31) Xie, Z.; Markus, T. Z.; Cohen, S. R.; Vager, Z.; Gutierrez, R.; Naaman, R. Spin Specific Electron Conduction through DNA Oligomers. *Nano Letters* **2011**, *11*, 4652–4655.
- (32) Mondal, P. C.; Roy, P.; Kim, D.; Fullerton, E. E.; Cohen, H.; Naaman, R. Photospintronics: Magnetic Field-Controlled Photoemission and Light-Controlled Spin Transport in Hybrid Chiral Oligopeptide-Nanoparticle Structures. *Nano Letters* **2016**, *16*, 2806–2811.
- (33) Banerjee-Ghosh, K.; Dor, O. B.; Tassinari, F.; Capua, E.; Yochelis, S.; Capua, A.; Yang, S.-H.; Parkin, S. S. P.; Sarkar, S.; Kronik, L. et al. Separation of Enantiomers by Their Enantiospecific Interaction with Achiral Magnetic Substrates. *Science* **2018**, *360*, 1331–1334.
- (34) Mentovich, E.; Belgorodsky, B.; Gozin, M.; Richter, S.; Cohen, H. Doped Biomolecules in Miniaturized Electric Junctions. *J. Am. Chem. Soc.* **2012**, *134*, 8468–8473.
- (35) Amdursky, N.; Sepunaru, L.; Raichlin, S.; Pecht, I.; Sheves, M.; Cahen, D. Electron Transfer Proteins as Electronic Conductors: Significance of the Metal and Its Binding Site in the Blue Cu Protein, Azurin. *Advanced Science* **2015**, *2*, 1400026.
- (36) Yu, X.; Lovrincic, R.; Sepunaru, L.; Li, W.; Vilan, A.; Pecht, I.; Sheves, M.; Cahen, D. Insights into Solid-State Electron Transport through Proteins from Inelastic Tunneling Spectroscopy: The Case of Azurin. *ACS Nano* **2015**, *9*, 9955–9963.

- (37) Zwolak, M.; Di Ventra, M. *Colloquium* : Physical Approaches to DNA Sequencing and Detection. *Rev. Mod. Phys.* **2008**, *80*, 141–165.
- (38) Migliore, A.; Nitzan, A. Nonlinear Charge Transport in Redox Molecular Junctions: A Marcus Perspective. *ACS Nano* **2011**, *5*, 6669–6685.
- (39) Migliore, A.; Nitzan, A. Irreversibility and Hysteresis in Redox Molecular Conduction Junctions. *J. Am. Chem. Soc.* **2013**, *135*, 9420–9432.
- (40) Craven, G. T.; Nitzan, A. Electron Transfer Across a Thermal Gradient. *Proc. Nat. Acad. Sci.* **2016**, *113*, 9421–9429.
- (41) Craven, G. T.; Nitzan, A. Electrothermal Transistor Effect and Cyclic Electronic Currents in Multithermal Charge Transfer Networks. *Phys. Rev. Lett.* **2017**, *118*, 207201.
- (42) Nitzan, A. A Relationship between Electron-Transfer Rates and Molecular Conduction. *J. Phys. Chem. A* **2001**, *105*, 2677–2679.
- (43) Albinsson, B.; Mårtensson, J. Long-Range Electron and Excitation Energy Transfer in Donor-Bridge-Acceptor Systems. *J. Photochem. Photobiol. C* **2008**, *9*, 138 – 155.
- (44) Jortner, J.; Bixon, M.; Langenbacher, T.; Michel-Beyerle, M. E. Charge Transfer and Transport in DNA. *Proc. Nat. Acad. Sci.* **1998**, *95*, 12759–12765.
- (45) Bixon, M.; Giese, B.; Wessely, S.; Langenbacher, T.; Michel-Beyerle, M. E.; Jortner, J. Long-Range Charge Hopping in DNA. *Proc. Nat. Acad. Sci.* **1999**, *96*, 11713–11716.
- (46) Bixon, M.; Jortner, J. Long-Range and Very Long-Range Charge Transport in DNA. *Chem. Phys.* **2002**, *281*, 393 – 408.
- (47) Sumi, H.; Kakitani, T. Unified Theory on Rates for Electron Transfer Mediated by a Midway Molecule, Bridging between Superexchange and Sequential Processes. *J. Phys. Chem. B* **2001**, *105*, 9603–9622.



- (48) Saito, K.; Sumi, H. Unified Expression for the Rate Constant of the Bridged Electron Transfer Derived by Renormalization. *J. Chem. Phys.* **2009**, *131*, 134101.
- (49) Leijnse, M.; Wegewijs, M. R. Kinetic Equations for Transport Through Single-Molecule Transistors. *Phys. Rev. B* **2008**, *78*, 235424.
- (50) Koller, S.; Grifoni, M.; Leijnse, M.; Wegewijs, M. R. Density-Operator Approaches to Transport Through Interacting Quantum Dots: Simplifications in Fourth-Order Perturbation Theory. *Phys. Rev. B* **2010**, *82*, 235307.
- (51) Nitzan, A.; Galperin, M. Kinetic Schemes in Open Interacting Systems. *J. Phys. Chem. Lett.* **2018**, *9*, 4886–4892.
- (52) Haug, H.; Jauho, A.-P. *Quantum Kinetics in Transport and Optics of Semiconductors*; Springer Series in Solid-State Sciences; Springer-Verlag: Berlin Heidelberg, 1996; Vol. 123.
- (53) Chen, F.; Ochoa, M. A.; Galperin, M. Nonequilibrium Diagrammatic Technique for Hubbard Green Functions. *J. Chem. Phys.* **2017**, *146*, 092301.
- (54) Yeganeh, S.; Ratner, M. A.; Galperin, M.; Nitzan, A. Transport in State Space: Voltage-Dependent Conductance Calculations of Benzene-1,4-dithiol. *Nano Letters* **2009**, *9*, 1770–1774.
- (55) White, A. J.; Tretiak, S.; Galperin, M. Raman Scattering in Molecular Junctions: A Pseudoparticle Formulation. *Nano Letters* **2014**, *14*, 699–703.
- (56) Miwa, K.; Najarian, A. M.; McCreery, R. L.; Galperin, M. Hubbard Nonequilibrium Green’s Function Analysis of Photocurrent in Nitroazobenzene Molecular Junction. *J. Phys. Chem. Lett.* **2019**, *10*, 1550–1557.

- (57) Miwa, K.; Imada, H.; Imai-Imada, M.; Kimura, K.; Galperin, M.; Kim, Y. Many-Body State Description of Single-Molecule Electroluminescence Driven by a Scanning Tunneling Microscope. *Nano Letters* **2019**, *19*, 2803–2811.
- (58) Kimura, K.; Miwa, K.; Imada, H.; Imai-Imada, M.; Kawahara, S.; Takeya, J.; Kawai, M.; Galperin, M.; Kim, Y. Selective Triplet Exciton Formation in a Single Molecule. *Nature* **2019**,
- (59) Mukamel, S. *Principles of Nonlinear Optical Spectroscopy*; Oxford Series in Optical and Imaging Sciences; Oxford University Press, 1995; Vol. 6.
- (60) Hubbard, J. Electron Correlations in Narrow Energy Bands. V. A Perturbation Expansion About the Atomic Limit. *Proc. Roy. Soc. A* **1967**, *296*, 82–99.
- (61) Izyumov, Y. A.; Skryabin, Y. N. *Statistical Mechanics of Magnetically Ordered Systems*; Consultants Bureau: New York and London, 1988.
- (62) Ovchinnikov, S. G.; Val'kov, V. V. *Systems Operators in the Theory of Strongly Correlated Electrons*; Imperial College Press, 2004.
- (63) Sandalov, I.; Johansson, B.; Eriksson, O. Theory of Strongly Correlated Electron Systems: Hubbard-Anderson Models from an Exact Hamiltonian, and Perturbation Theory near the Atomic Limit Within a Nonorthogonal Basis Set. **2003**, *94*, 113–143.
- (64) Fransson, J. Nonequilibrium Theory for a Quantum Dot with Arbitrary On-Site Correlation Strength Coupled to Leads. *Phys. Rev. B* **2005**, *72*, 075314.
- (65) Sandalov, I.; Nazmitdinov, R. G. Nonlinear Transport at the Strong Intra-Dot Coulomb Interaction. *J. Phys.: Condens. Matter* **2006**, *18*, L55–L61.
- (66) Sandalov, I.; Nazmitdinov, R. G. Shell Effects in Nonlinear Magnetotransport Through Small Quantum Dots. *Phys. Rev. B* **2007**, *75*, 075315.

- (67) Galperin, M.; Nitzan, A.; Ratner, M. A. Inelastic Transport in the Coulomb Blockade Regime Within a Nonequilibrium Atomic Limit. *Phys. Rev. B* **2008**, *78*, 125320.
- (68) Fransson, J. *Non-Equilibrium Nano-Physics - A Many-Body Approach*; Springer-Verlag, 2010.
- (69) Miwa, K.; Chen, F.; Galperin, M. Towards Noise Simulation in Interacting Nonequilibrium Systems Strongly Coupled to Baths. *Sci. Rep.* **2017**, *7*, 9735.
- (70) Chen, F.; Miwa, K.; Galperin, M. Current-Induced Forces for Nonadiabatic Molecular Dynamics. *J. Phys. Chem. A* **2019**, *123*, 693–701.
- (71) Chen, F.; Miwa, K.; Galperin, M. Electronic Friction in Interacting Systems. *J. Chem. Phys.* **2019**, *150*, 174101.
- (72) Galperin, M.; Ratner, M. A.; Nitzan, A. Comment on “Frequency-Domain Stimulated and Spontaneous Light Emission Signals at Molecular Junctions” [J. Chem. Phys. 141, 074107 (2014)]. *J. Chem. Phys.* **2015**, *142*, 137101.
- (73) Galperin, M. Photonics and Spectroscopy in Nanojunctions: A Theoretical Insight. *Chem. Soc. Rev.* **2017**, *46*, 4000–4019.
- (74) Galperin, M.; Ratner, M. A.; Nitzan, A. Published: arXiv:1503.03890.

## Graphical TOC Entry

